NANOENGINEERED GLASS FIBER REINFORCED COMPOSITE LAMINATES WITH INTEGRATED MULTIFUNCTIONALITY

Title: **Nanoengineered Glass Fiber Reinforced Composite Laminates with Integrated Multifunctionality**

Authors: Palak Patel[1]
Carolina Furtado[1]
Megan Cooper[1]
Luiz Acauan[1]
Stepan Lomov[2]
Iskander Akhatov[2]
Sergey Abaimov[2]
Jeonyoon Lee[1]
Brian Wardle[1]

[1] Massachusetts Institute of Technology, Cambridge, Massachusetts, United States
[2] Skolkovo Institute of Science and Technology, Moscow, Russia

ABSTRACT

Combining one or more functional capabilities of subsystems within a structure can provide system-level savings, particularly for weight-critical applications such as air and space vehicles. Nanoengineering presents a significant opportunity for additional functionalities on the nanoscale without the necessity to modify shape, design, or load carrying capacity of the structure. Here, an integrated-multifunctional nano-engineered system was preliminarily studied in composite laminate structures. The study would support the exploration of a system designed to serve independent yet synergistic functionalities in life-cycle enhancements, energy savings during manufacturing, in-situ cure (manufacturing) monitoring, and in-service damage sensing. For the preliminary study, an integrated multifunctional composite (IMC) laminate was created via aligned nanofiber introduction into the composite interlaminar region and the laminate surfaces of Hexcel E-glass/913 unidirectional glass fiber prepreg. Various heights ranging from 10 - 40 μm-tall vertically aligned carbon nanotube (VA-CNT) arrays, as well as patterned and buckled VA-CNT architectures, were used to reinforce the weak interlaminar regions within the laminates showing a ~ 4 - 5% increase in short beam strength of VA-CNT reinforced specimens hence demonstrating interlaminar enhancement for life-cycle advancements. The same layers, being electrically conductive, can provide several additional multifunctionalities.

[1] Massachusetts Institute of Technology, 77 Massachusetts Avenue, Cambridge, Massachusetts 02139, U.S.A. Email: wardle@mit.edu
[2] Skolkovo Institute of Science and Technology, Bolshoy Boulevard 30, Building 1, Moscow, 121205, Russia. Email: s.abaimov@skoltech.ru

INTRODUCTION

Lightweight heterogenous materials, like composites, have allowed the design and development of innovative aerospace components. While these heterogenous composite materials are advantageous from a reduction of weight point of view, they may be susceptible to detrimental failure modes in weaker regions like the interlaminar region. The use of nano-materials to reinforce the interlaminar region of composites provides a nano-scale solution to reinforcing the weaker regions of a composite without increasing the thickness of the interlaminar region [1]. The use of carbon nanotubes (CNTs) to reinforce the interlaminar region of composites has proven successful in carbon fiber laminates, showing increases in shear strength when compared to unreinforced laminates with insignificant changes in interlaminar thickness between reinforced and unreinforced interlaminar regions [1-8]. Vertically aligned carbon nanotubes (VA-CNTs) placed to reinforce the interlaminar region are known as nanostitch and different morphologies have been explored. Both studies of VA-CNTs [1-6] and buckled VA-CNTs [7-8] had shown increased interlaminar, intralaminar, and laminate-level strengths, including fatigue, due to the nanoscale reinforcement architectures.

Besides reinforcing applications, nano-engineering of these lightweight materials allows for the addition of multifunctionalities with little or no increase in weight while adding multiple advantageous functionalities besides the primary structural function. While nano-engineered multifunctional capabilities of structural materials have been explored individually, like life-cycle enhancement [1-15], energy saving during manufacturing [9-14], sensing and control [9], in-situ cure monitoring [11-13], and de-icing [15], the integration of these multifunctionalities into one engineered composite has not been undertaken. In this paper, a preliminary study of one such integrated multifunctional composite (IMC) was performed by the nano-engineering of laminates based on Hexcel E-glass/913 unidirectional glass fiber prepreg with the focus on investigating the effect of VA-CNT interlaminar reinforcement and CNT commercial film on the quality and strength of the composite laminates. Evaluating the multifunctionalities is future work as the structural function is shown to be more than maintained, and is in fact enhanced, in this paper.

INTEGRATED MULTIFUNCTIONAL COMPOSITE (IMC) FABRICATION

IMC fabrication is described here, including VA-CNT synthesis, integration of commercial and VA-CNTs into the glass fiber reinforced polymer (GFRP) prepreg composites including curing and the overall test matrix.

Synthesis of VA-CNTs

To nanoengineer the composite, carbon nanotubes (CNTs) were introduced to the glass fiber composite prepreg system between the plies. In this work, three types of CNT architectures were utilized for interlaminar reinforcement and integrated into different specimens. Vertically aligned carbon nanotubes (VA-CNTs) were synthesized according to standard procedures and are referred to as nanostitch 1.0 [1-6]. VA-CNTs in square patterned arrays are referred to as patterned nanostitch 1.0. A novel nanoengineered hierarchical layered architecture of densely synthesized VA-CNTs that consist of buckled arrays of VA-CNTs are referred to a nanostitch 2.0 [7-8].

A thermal catalytic chemical vapor deposition (CVD) process was utilized to synthesize all three CNT architectures. Silicon wafer substrates of dimensions 30 mm x 40 mm were placed in a quartz tube furnace with an inner diameter of 44 mm at atmospheric pressure as previously described [1]. The silicon wafer used for nanostitch 1.0 had uniform layers of deposited catalyst (1 nm of Fe on top of 10 nm of Al2O3 on the silicon wafer). Patterned nanostitch 1.0 and nanostitch 2.0 were grown on wafers with a patterned deposition of catalyst of the same thickness. The pattern was created by shadow masking wafers with a nickel mesh before the catalyst deposition. The pattern created VA-CNT squares of dimensions 49 μm x 49 μm with a 14 μm gap between squares. While the forests of CNTs grown for nanostitch 1.0 and patterned nanostitch 1.0 were integrated in the interlaminar region of the composites as grown, the CNT forests used for nanostitch 2.0 were buckled to form denser forests as seen in Figure 1. The buckling process involved placing a bare silicon wafer on top of the silicon wafer substrate with patterned CNT and applying uniform pressure by hand to buckle the VA-CNTs to form the architectures for nanostitch 2.0. Nanostitch 1.0 with CNT array heights of 10, 20, 30 and 40 μm were grown. Patterned nanostitch 1.0 of CNT heights 20 and 40 μm, and nanostitch 2.0, initially grown with heights of 20 and 40 μm and buckled down to lower heights, were integrated in composite specimens with the purpose of comparing their properties with those of baseline non-reinforced composites.

Fabrication of Nanoengineered Glass Fiber Laminates

Hexcel NVE 913, an epoxy E-glass unidirectional autoclave-grade prepreg, was used to form the composite. The laminate assembly consisted of a quasi-isotropic 16 ply lay-up. The different VA-CNT architectures (nanostitch 1.0, patterned nanostitch 1.0, and nanostitch 2.0) were integrated into the prepreg system by manual transfer between the prepreg plies during the laminate lay-up procedure at room temperature, creating the IMC laminates. Two laminate lay-ups for plate dimensions 150 mm x 150 mm were performed in the following orientations:

- Baseline plate: $[0/90/45/-45]_{2s}$ quasi-isotropic 16-ply laminate.
- CNT plate: $[0/90/45/-45]_{2s}$ quasi-isotropic 16-ply laminate with six regions of specimens (size 30 x 40 mm) with varying VA-CNT architectures in each specimen. Specimens 1 to 4 had various CNT architectures placed in 5 central interlaminar regions, as seen in Figure 2,

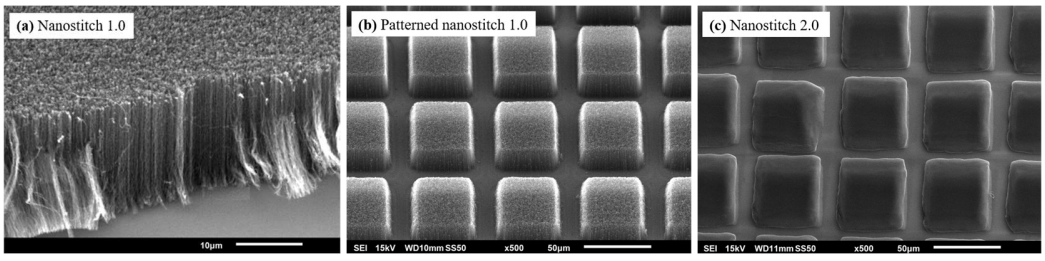

Figure 1. Scanning electron micrographs of CNT architectures used in this study: (a) VA-CNTs in nanostitch 1.0 configuration, (b) VA-CNTs in patterned nanostitch 1.0 configuration, and (c) buckled VA-CNTs in nanostitch 2.0 configuration.

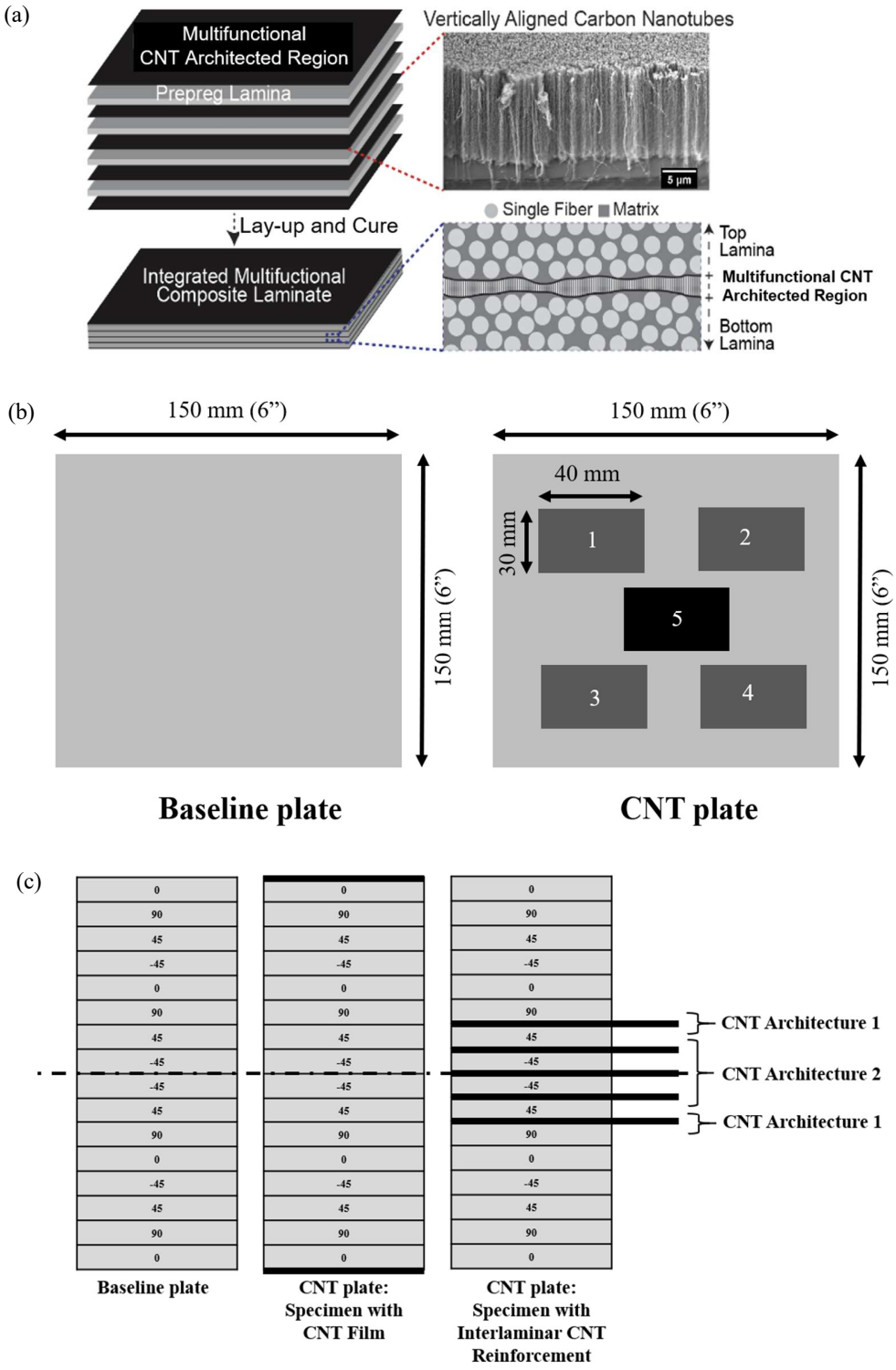

Figure 2. Integrated multifunctional composites (IMC) manufacturing: (a) Schematics of IMC laminate, (b) Placement of specimens in the baseline and CNT plates, and (c) Quasi-isotropic 16- ply laminate lay-up of baseline plate and CNT plate with ply orientation and position of interlaminar multifunctional CNT architectures. Architectures explained in Table 1.

TABLE 1. VA-CNT ARCHITECTURES IN PLATES AND SPECIMENS.

Plate Name	Specimen Name	Multifunctional Nanostructured reinforcement Architecture	Multifunctional Nanostructured reinforcement Architecture 1: CNT height (μm)	Multifunctional Nanostructured reinforcement Architecture 2: CNT height (μm)
Baseline Plate	Baseline Specimen	None	None	None
CNT Plate	CNT Specimen Baseline	None	None	None
	CNT Specimen 1	Nanostitch 1.0	10	20
	CNT Specimen 2	Nanostitch 1.0	30	40
	CNT Specimen 3	Patterned Nanostitch 1.0	20	40
	CNT Specimen 4	Nanostitch 2.0	20	40
	CNT Specimen 5	Commercial CNT film	None	None

to reinforce the center of the laminate. The specific VA-CNT architectures in each specimen can be found in Table 1. Specimen 5 had no CNTs placed at the interfaces, but had a randomly-oriented commercial CNT film (Tortech, CNTM4) of thickness 16 μm placed on the top and bottom of the lay-up. Specimen 6 was a region of the CNT plate which had no CNTs at any of the interlaminar regions.

Both of the laminates were cured after the lay-up following the manufacturer recommended cure cycle.

- Vacuum at 0.7 bar (20 in Hg) at the start. Increase pressure to 6 – 7 bar (85-100 psig) and hold throughout the cure cycle. Vent vacuum when the pressure inside chamber reaches 1.4 bar (20 psig). Increase temperature at a steady rate of not more than 5°C/min (9 °F/min) till 90°C (195°F).
- Dwell - Hold temperature at 90°C (195°F) for 30 minutes.
- Increase temperature at a steady rate of not more than 5°C/min (9°F/min) till the temperature reaches 120 – 130°C (250 – 265°C) and hold for 60 minutes.
- Decrease the temperature at ≤ 3°C/min (5°F/min) and then release pressure to 0 bar (0 psig) when the temperature reaches 65°C (150°F).

Both laminates were cured in the same autoclave cycle, under the same conditions for consistency of manufacturing.

CHARACTERIZATION AND EXPERIMENTAL RESULTS

As the first step in studying multifunctionality of CNT-containing interlaminar regions, we assessed here any effects of the CNT integration on the laminate characteristics, including interlaminar thickness and void content. Both should be similar to the baseline material without CNT integration to maintain the overall primary structural function.

Since some methods of integrating multifunctionalities to composite systems degrades the strength of the composite, tests to evaluate the interlaminar shear strength (ILSS) via short beam shear strength testing were performed.

Void Characterization: X-Ray Micro-Computed Tomography (μ-CT)

Voids can form in the interlaminar region of the composite, due to uneven prepreg surfaces and entrapped air, or less commonly in the intralaminar region within the ply. Even low void percentages can severely degrade the strength and durability of the composite [16]. To ensure that the plate with the integrated VA-CNT nanostructured reinforcement was able to maintain a comparable quality to the baseline plate, a void characterization study was performed. Micro-computed tomography's (μ-CT) non-destructive X-ray imaging technique allowed the composite to be characterized for voids that may exist post cure. The scans were performed using a ZEISS Versa 520 micro-CT system which scanned the sample using the Scout-and-ScanTM Control System software and imaged slices of the sample's cross section. The images were reconstructed using Scout-and-ScanTM Control System Reconstructor software with manual centering. The scans were conducted on a sample of dimensions 10 mm x 10 mm x thickness of composite post cure with a voxel size of 1.2 μm. In the μ-CT images, the lighter the grey-scaled regions, the denser the material that the x-rays passed through. Hence fibers and resin show up as lighter on the grey-scale, while voids appear darker or almost black.

Representative images of the baseline specimen and CNT integrated specimens are shown in Figure 3. As can be seen in the μ-CT scans, the lightest grey represents the glass fiber in the matrix of medium grey resin. The CNTs in the interlaminar regions are not easily distinguishable from the resin as this region is a nanocomposite of CNTs and polymer resin, with both having similar x-ray contrast. No voids were visible in any of the specimen configurations hence it could be concluded that the quality and void characteristics of the CNT integrated specimens were comparable to the baseline specimen.

Interlaminar Thickness: Optical Microscopy

Maintaining the interlaminar thickness of the composites with the integrated CNTs in the interlaminar region is imperative in comparative studies between baseline composites and IMCs. The inclusion of multifunctionalities in composites using nano-scaled materials should ideally be done without any significant change in the thickness of the cured composite, as changes in composite thickness are related to changes in resin content and/or location within the laminate that can affect the performance of the material. The interlaminar regions of the manufactured specimens were visualized using an optical microscope. The specimens were cut using a diamond-grit belt saw and the surface to be imaged was grinded and then polished with suspension particle size of 1 μm followed by 0.2 μm. A Carl Zeiss Axiotech 25 HD optical microscope was used at a magnification of 50x in the bright field to image the interlaminar regions of all specimens.

The interlaminar regions of the specimen slightly varied in thickness due to variability in fiber placement in the prepreg plies. As shown in representative interlaminar regions in Figure 4, the thickness of the interlaminar region in the CNT

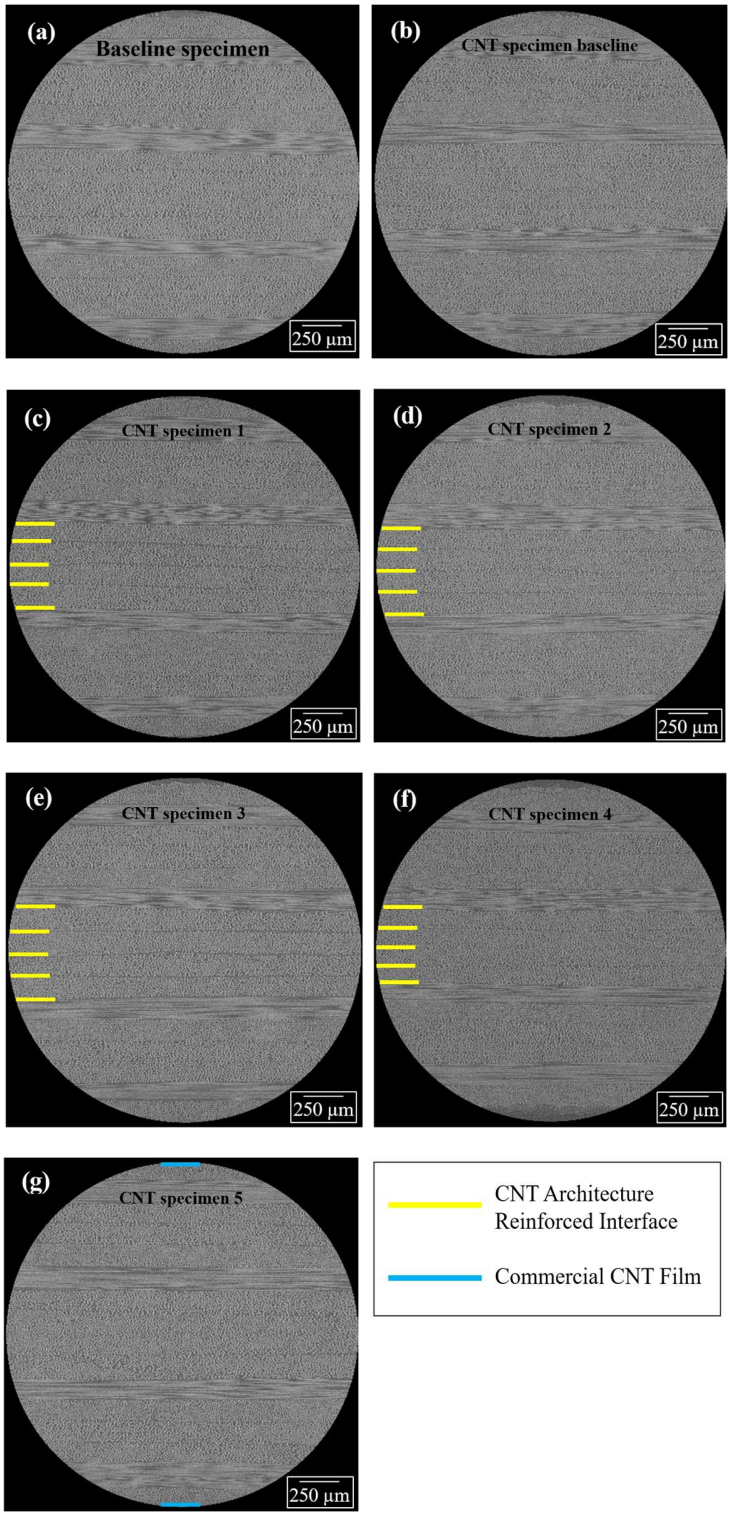

Figure 3. X-ray micro-computed tomography images of laminates: (a) baseline specimen, (b) CNT specimen baseline, (c) CNT specimen 1, (d) CNT specimen 2, (e) CNT specimen 3, (f) CNT specimen 4, and (g) CNT specimen 5. Glass fibers are imaged as light grey and the resin appears as a darker grey. Yellow lines annotate the CNT architecture reinforced interface locations and blue lines annotate the commercial CNT film's placement.

specimens (1.5-5 μm) remains within the range of the variability of the thickness of the baseline specimen's interlaminar region (1-5 μm). As shown in Figure 5, the thickness of the composites also did not increase significantly with the addition of the CNT interlaminar architectures and all laminates presented a comparable thickness. This suggests that the thickness of the composite is not expected to significantly increase with the incorporation of carbon nanotubes, even if they were placed in every interface. The commercial CNT film placed on the outer surfaces of CNT specimen 5 was fully impregnated by the resin of the prepreg and therefore increased the thickness of the laminate, but since the increase in thickness of the laminate is not related to the interfaces, it did not influence interface properties such as short beam shear strength as shown below.

Interlaminar Shear Strength via Short Beam Shear Test

The short beam shear strength test (SBS) was performed according to ASTM standard D2344 [17] to test the interlaminar shear strength (ILSS) of the laminate. Following the standard, SBS specimens of dimensions 12 mm x 4 mm x 2 mm (length x width x thickness) were cut out from the CNT plate and grinded to remove notches at the edges of the specimens that could act as a damage initiator leading to premature failure of the specimens. A Zwick/Roell Z010 mechanical testing machine was used to perform the test on a three-point bend fixture with a crosshead movement rate of 1 mm/min. The short beam shear strength (σSBS) is computed via:

$$\sigma_{SBS} = 0.75 \times \left(\frac{P_f}{w \times t}\right) \quad (1)$$

where P_f is the failure load, w is the width of the SBS specimen, and t is the thickness of the SBS specimen. Five SBS specimens per configuration (baseline specimen, CNT plate baseline specimen, and CNT specimens 1-5) were tested.

Figure 6 shows and compares the short beam strength of the baseline specimens and CNT architecture reinforced specimens. The baseline plate's specimens observed a short beam strength of 90.73 ± 2.22 MPa (mean and standard error) and the CNT plate's baseline specimens had a comparable strength of 92.49 ± 1.35 MPa and was consistent with the CNT plate's unreinforced specimen with commercial CNT film (CNT specimen 5) with a short beam strength of 91.78 ± 0.98 MPa. CNT specimen 1, reinforced with nanostitch 1.0 of 10 and 20 μm height, showed a statistically significant 4.91% increase in strength compared to the baseline with a short beam strength of 95.19 ± 0.90 MPa, while CNT specimen 2 with nanostitch 1.0 of 30 and 40 μm also showed a statistically significant 4.16% increase in strength compared to the baseline with a short beam strength of 94.50 ± 0.61 MPa. CNT specimen 3 with patterned nanostitch 1.0 with CNT heights of 20 and 40 μm and CNT specimen 4 with nanostitch 2.0 with 20 and 40 μm height CNTs buckled down had short beam strengths of 93.21 ± 0.87 MPa and 90.74 ± 0.32 MPa respectively. Taking into consideration the standard error, there was a statistically significant increase in the short beam strength of nanostitch 1.0 reinforced specimens in comparison to the baseline specimen, while nanostitch 2.0 maintained a comparable strength to the baseline specimen. The highest short beam shear strength was seen in CNT specimen 1 with nanostitch 1.0 of heights 10 and 20 μm.

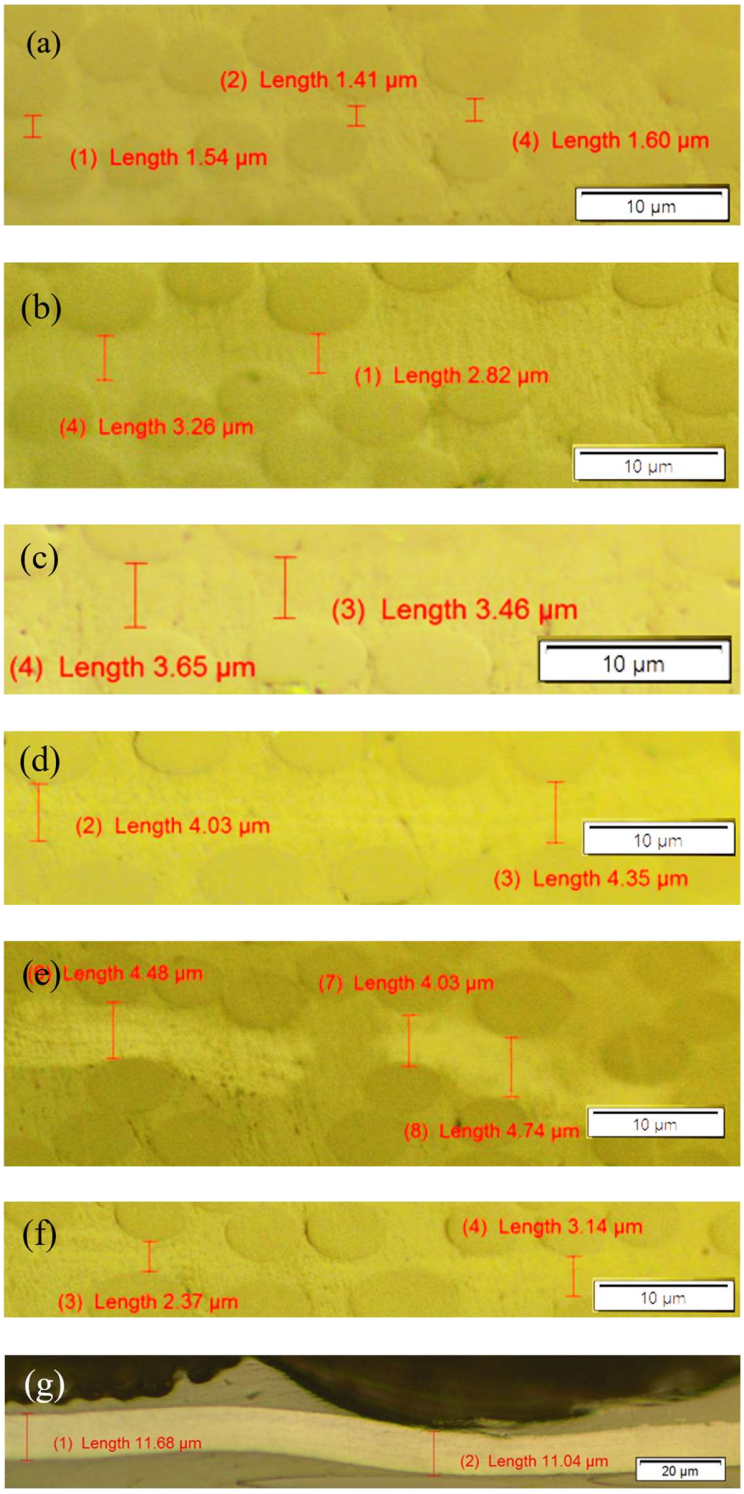

Figure 4. Optical micrographs of the interlaminar region and measured interlaminar thicknesses of the: (a) baseline specimen, (b) CNT specimen baseline, (c) CNT specimen 1 with nanostitch 1.0 of 20 µm height, (d) CNT specimen 2 with nanostitch 1.0 of 40 µm height, (e) CNT specimen 3 with patterned nanostitch 1.0 of 40 µm height, and (f) CNT specimen 4 with nanostitch 2.0 of 40 µm height, and the CNT film thickness of (g) CNT specimen 5 with commercial CNT film.

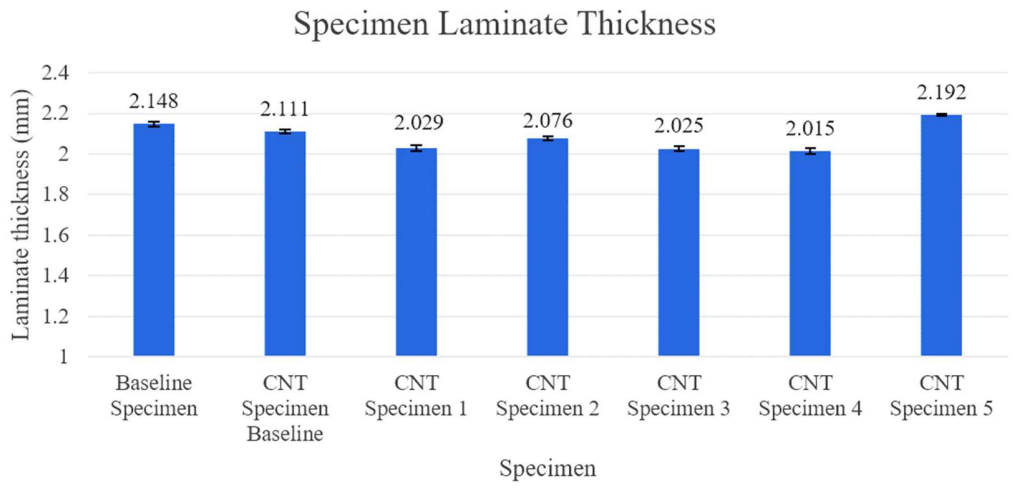

Figure 5. Specimen laminate thickness with standard error.

All tests were considered to have valid failure modes according to the ASTM standards [17]. The baseline specimens failed through the interlaminar region in long crack failures, as seen in Figure 7 (a), while the CNT-reinforced specimens deflected the crack through the plies from the reinforced interlaminar regions to the outer layers' interlaminar regions which were not reinforced with CNTs, as seen in Figure 7 (b) and (c). This damage state is representative of the reinforcing effect of integrating aligned CNT architectures into the interlaminar regions.

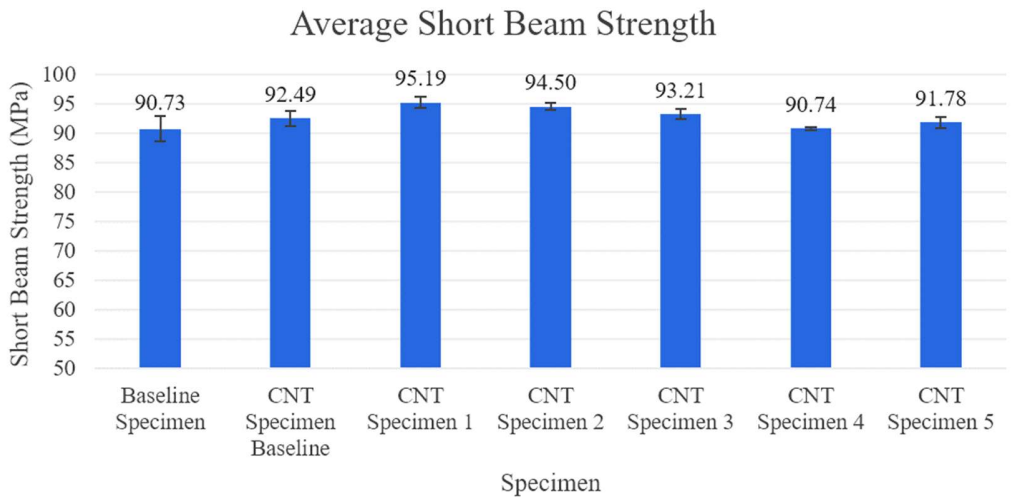

Figure 6. Average short beam strengths with standard error.

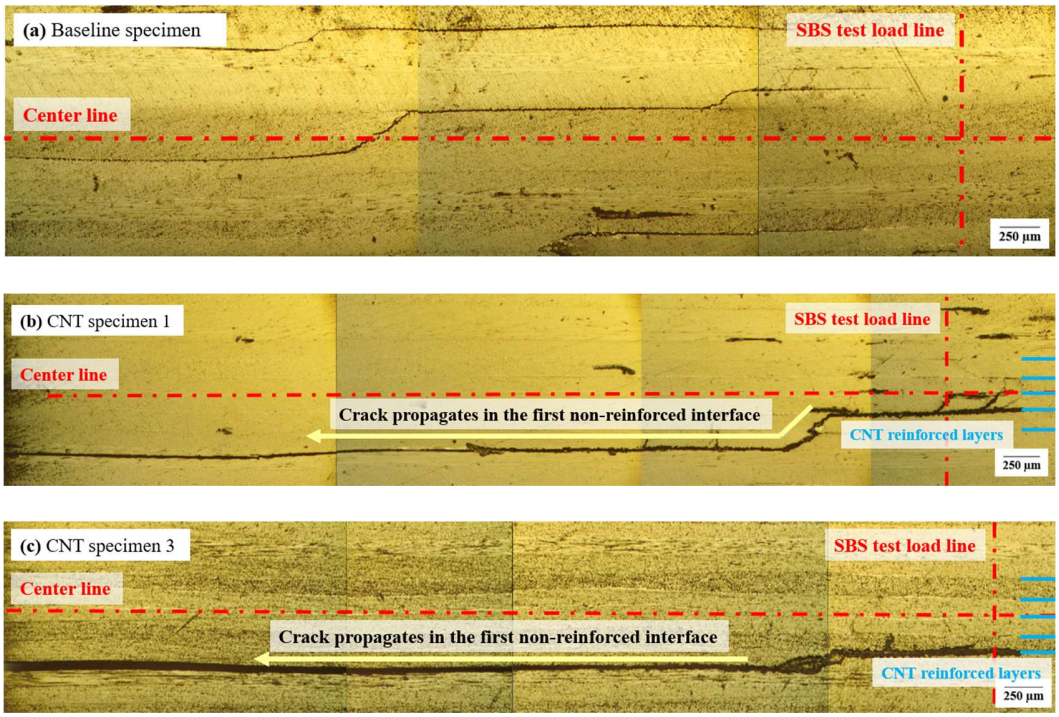

Figure 7. Representative short beam shear test post mortem cross sections for: (a) baseline specimen, (b) CNT specimen 1 with nanostitch 1.0 reinforced center layers, and (c) CNT specimen 3 with patterned nanostitch 1.0 reinforced center layers. Horizontal red center lines indicate the center lines of the specimen, the vertical red lines indicate the line of SBS test load application, and the blue lines indicate the layers with CNT reinforcement.

CONCLUSION

In this work, a study of the integration of multifunctionalities was explored by the strategic placement of aligned and randomly-oriented CNTs in the interlaminar region and surfaces, respectively, of glass fiber composite laminates. The resulting laminates were characterized and tested to ensure interlaminar characteristics and strengths were comparable to baseline glass fiber laminates. Three types of VA-CNTs and buckled CNT morphologies were investigated at heights varying from 10 – 40 µm. It was demonstrated that, while the interlaminar thicknesses of the reinforced regions remained unchanged, two CNT specimens that were reinforced with nanostitch 1.0 at 10 and 20 µm and nanostitch 1.0 at 30 and 40 µm resulted in effective reinforcement of the interlaminar region with statistically significant increase of 4.91% and 4.16% respectively in short beam strengths compared to the baseline. Moreover, the CNT reinforced interlaminar layers forced crack propagation to occur through the intralaminar region or through unreinforced interfaces, confirming the effectiveness of the CNT reinforcement technique. The commercial CNT films integrated in the outer surfaces of the laminates were shown to result in full impregnation of the CNT film, demonstrating its compatibility with the glass fiber composite. This will be further studied towards integrating additional multifunctionalities in the IMC laminates. These results strengthen the foundation for further exploration of the integration of multifunctionalities using nanostructured reinforcements in this particular glass fiber composite system.

ACKNOWLEDGEMENTS

This work was supported by the Skoltech NGP Program (Skoltech-MIT joint project "Multifunctional Fusion: Life-cycle enhancements via data-driven nanoengineering of advanced composite structures")

REFERENCES

1. R Guzman De Villoria, P Hallander, L Ydrefors, P Nordin, and BL Wardle. In-plane strength enhancement of laminated composites via aligned carbon nanotube interlaminar reinforcement. Composites Science and Technology, 133:33–39, 2016
2. Estelle Kalfon-Cohen, Reed Kopp, Carolina Furtado, Xinchen Ni, Albertino Arteiro, Gregor Borstnar, Mark N Mavrogordato, Ian Sinclair, S Mark Spearing, Pedro P Camanho, et al. Synergetic effects of thin plies and aligned carbon nanotube interlaminar reinforcement in composite laminates. Composites Science and Technology, 166:160–168, 2018.
3. Xinchen Ni and Brian L Wardle. Experimental investigation of interlaminar fracture micro-mechanisms of aligned carbon nanotube-reinforced aerospace laminated composites. In AIAA Scitech 2019 Forum, page 1201, 2019.
4. Xinchen Ni, Carolina Furtado, Nathan K Fritz, Reed Kopp, Pedro P Camanho, and Brian L Wardle. Interlaminar to intralaminar mode I and II crack bifurcation due to aligned carbon nanotube reinforcement of aerospace-grade advanced composites. Composites Science and Technology, 190:108014, 2020.
5. Xinchen Ni, Estelle Kalfon-Cohen, Carolina Furtado, Reed Kopp, Nathan K Fritz, A Arteiro, G Valdes, T Hank, G Borstnar, M Mayrogordato, et al. Interlaminar reinforcement of carbon fiber composites using aligned carbon nanotubes. In submitted to the 21st International Conference on Composite Materials (ICCM), Xi'an, China, 2017.
6. Xinchen Ni, Carolina Furtado, Estelle Kalfon-Cohen, Yue Zhou, Gabriel A Valdes, Travis J Hank, Pedro P Camanho, and Brian L Wardle. Static and fatigue interlaminar shear reinforcement in aligned carbon nanotube-reinforced hierarchical advanced composites. Composites Part A: Applied Science and Manufacturing, 120:106–115, 2019.
7. Xinchen Ni, Luiz H Acauan, and Brian L Wardle. Coherent nanofiber array buckling-enabled synthesis of hierarchical layered composites with enhanced strength. Extreme Mechanics Letters, 39:100773, 2020.
8. Xinchen Ni and Brian L Wardle. Aerospace-grade advanced composites with buckling-densified aligned carbon nanotubes interlaminar reinforcement. In AIAA Scitech 2020 Forum, page 0156, 2020.
9. Jeonyoon Lee, Itai Y Stein, Seth S Kessler, and Brian L Wardle. Aligned carbon nanotube film enables thermally induced state transformations in layered polymeric materials. ACS applied materials & interfaces,7(16):8900–8905, 2015.
10. Jeonyoon Lee, Xinchen Ni, Frederick Daso, Xianghui Xiao, Dale King, Jose Sánchez Gómez, Tamara Blanco Varela, Seth S Kessler, and Brian L Wardle. Advanced carbon fiber composite out-of-autoclave laminate manufacture via nanostructured out-of-oven conductive curing. Composites Science and Technology, 166:150–159, 2018.
11. Jeonyoon Lee, Frederick Daso, Seth S Kessler, and Brian L Wardle. Carbon fiber prepreg composite laminates cured via conductive curing using nanoengineered nanocomposite heaters
12. Jeonyoon Lee and Brian L Wardle. Nanoengineered in situ cure status monitoring technique based on carbon nanotube network. In AIAA Scitech 2019 Forum, page 1199, 2019.
13. Jeonyoon Lee, Itai Y Stein, Erica F Antunes, Seth S Kessler, and Brian L Wardle. Out-of-oven curing of polymeric composites via resistive microheaters comprised of aligned carbon nanotube networks. 2015.
14. Jeonyoon Lee, Seth S Kessler, and Brian L Wardle. Void-free layered polymeric architectures via capillary-action of nanoporous films. Advanced Materials Interfaces, 7(4):1901427, 2020.
15. Jeonyoon Lee, Christopher J Brampton, Christopher R Bowen, Brian L Wardle, and Hyunsun A Kim. Investigation of aligned conductive polymer nanocomposites for actuation of bistable laminates. In 23rd AIAA/AHS Adaptive Structures Conference, page 1725, 2015.

16. L. Farhang, Void Evolution during Processing of Out-of-Autoclave Prepreg Laminates. PhD thesis, University of British Columbia, 10 2004.
17. STM D 2344 / D 2344M-16, “Standard Test Method for Short Beam Strength of Polymer Matrix Composite Materials and Their Laminates,” West Conshohocken, PA: ASTM International.